PNAS
www.pnas.org

Supplementary Information for

FGF23 contains two distinct high-affinity binding sites enabling bivalent interactions with α-Klotho

Yoshihisa Suzuki, Ekaterina Kuzina, Seong J. An, Francisco Tome, Jyotidarsini Mohanty, Wenxue Li, Sangwon Lee, Yansheng Liu, Irit Lax and Joseph Schlessinger

Corresponding author: Joseph Schlessinger
E-mail: joseph.schlessinger@yale.edu

This PDF file includes:

Figures S1 to S10

www.pnas.org/cgi/doi/10.1073/pnas.2018554117

Supplementary Appendix

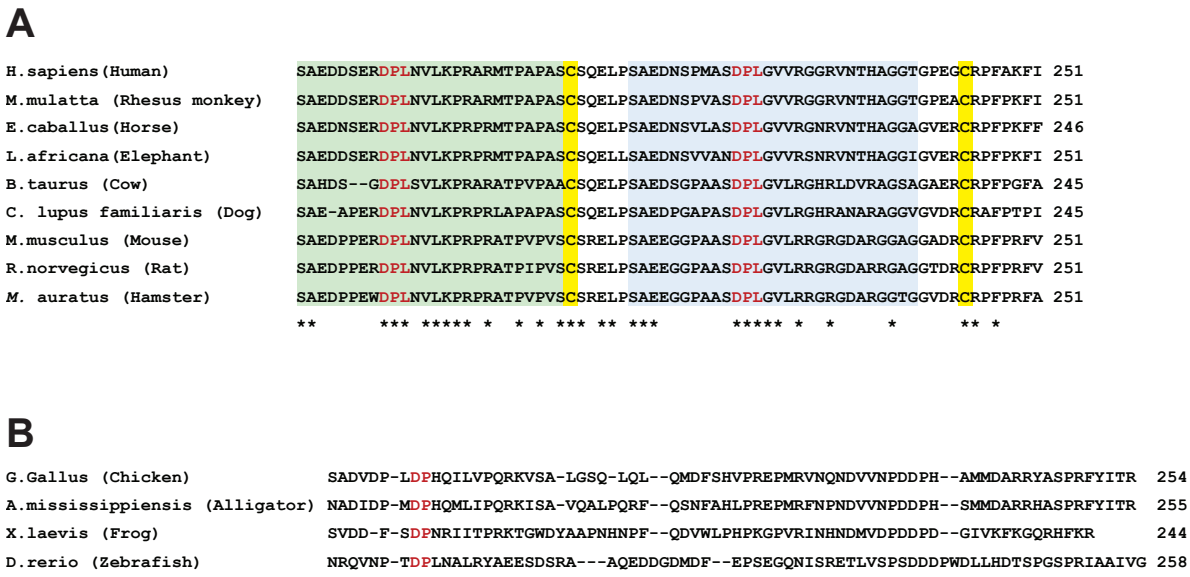

Figure S1.
A. Amino acid sequence alignments of the C-terminal tails of FGF23 from various mammalian species. Repeat 1(R1) is highlighted in green, repeat 2 (R2) is highlighted in light blue, conserved cysteine residues are highlighted in yellow. The conserved DPL motif, which is critical for Klotho binding, is colored red**. B.** Amino acid sequence alignments of the C-terminal tails of FGF23 from other vertebrate species. In vertebrates other than mammals only two amino acids (DP) of the DPL motif are conserved and they are highlighted in red.

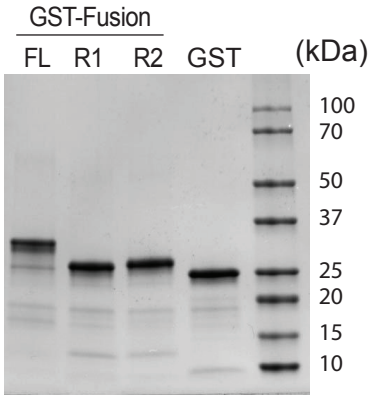

Figure S2.
SDS-PAGE analysis of GST-FL, GST-R1, GST-R2 and GST.

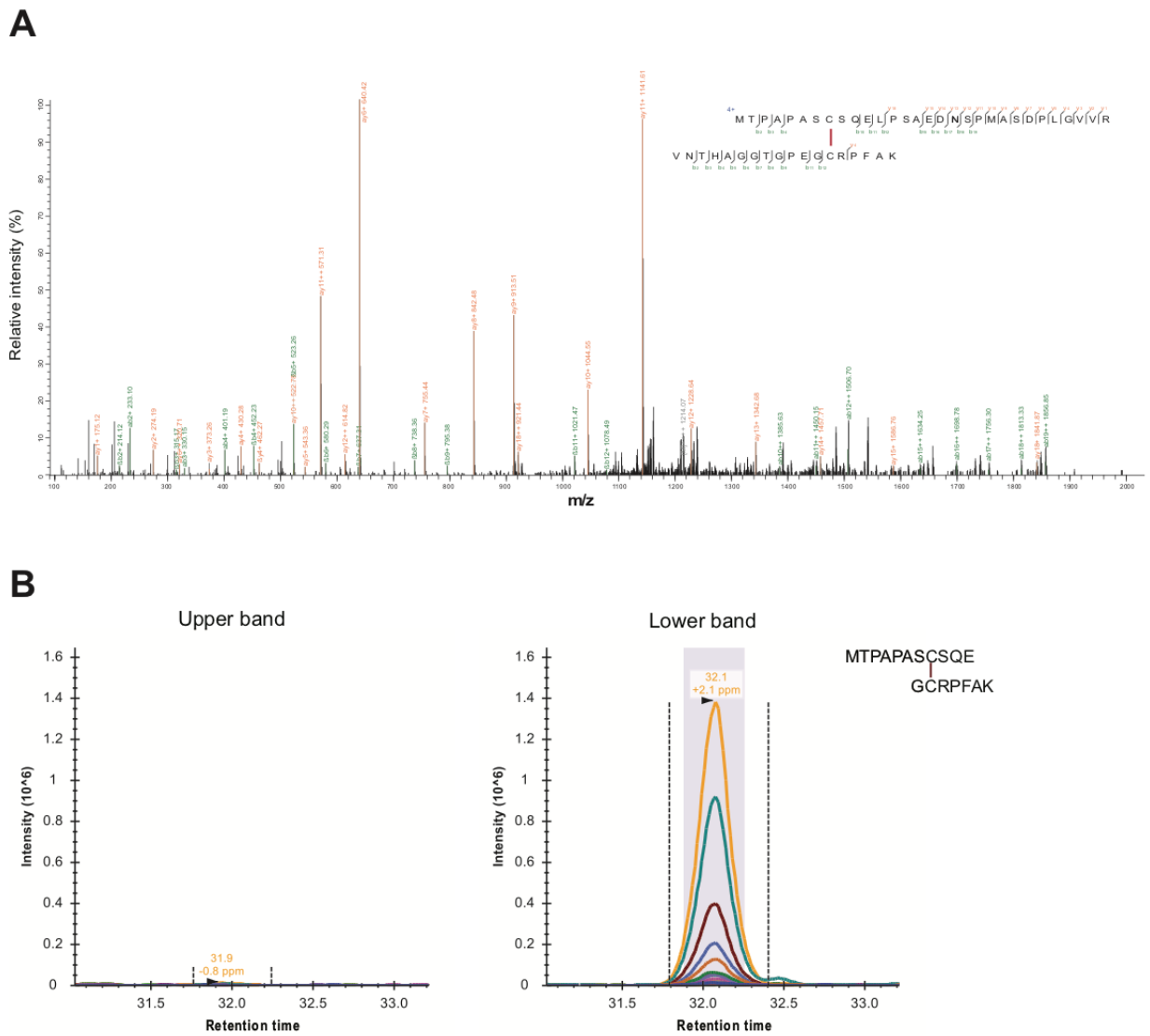

Figure S3.

A. MS/MS fragmentation spectrum directly identified the digested fragment of FGF23 expressed in E. coli that contains the Cys206-Cys244 disulfide bond. The corresponding b and y ions mapping to respective fragment ions of the two peptides forming disulfide-linked peptide were highlighted (b ions, green, y ions, orange). **B.** Relative amounts of bridged vs non-bridged Cys206 and Cys244 in various FGF23 samples presented by PRM measurement. The unique MS2 ions of high resolution (different colored traces) were manually inspected with Skyline visualization.

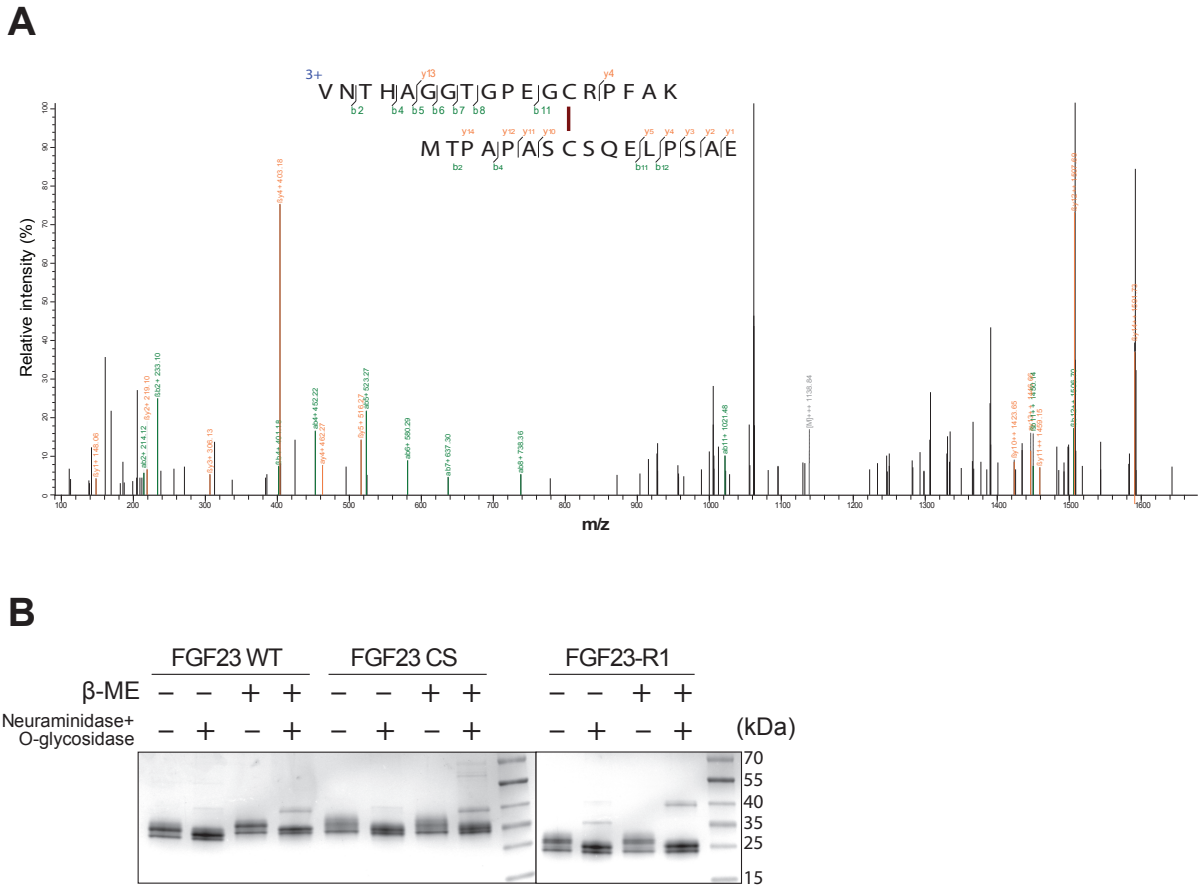

Figure S4.

A. MS/MS fragmentation spectrum directly identified the fragment of FGF23 expressed in Expi293F cells (FGF23-WT) containing the Cys206-Cys244 disulfide bond. The corresponding b and y ions mapping to respective fragment ions of the two peptides forming disulfide-linked peptide were highlighted (b ions, green, y ions, orange). **B.** SDS-PAGE analysis of purified FGF23-WT, FGF23-CS (C206S/C244S mutant), and FGF23-R1 (variant lacking C-terminal residues C206-I251),treated with *O*-glycosidase and α-(2→3,6,8,9)-neuraminidase. All FGF23 variants were expressed in Expi293F cells.

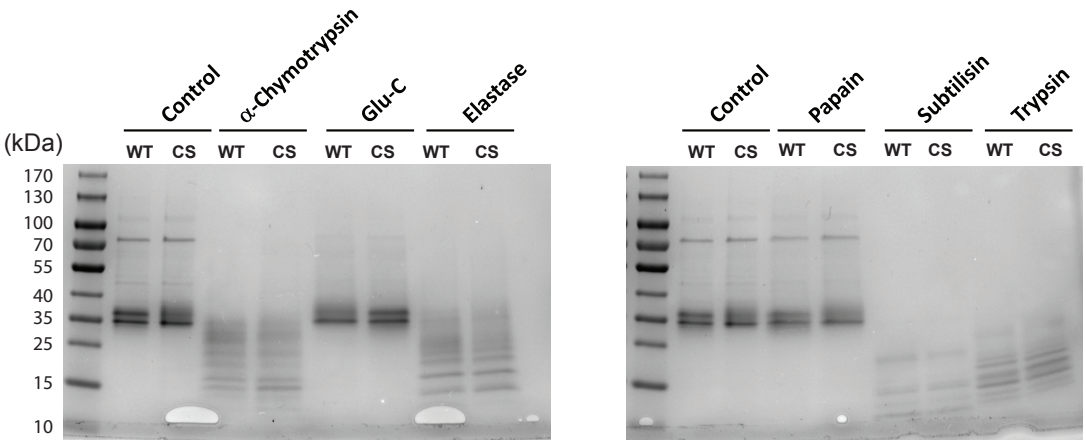

Figure S5.
SDS-PAGE analysis of FGF23-WT and FGF23-CS expressed and purified from Expi293F cells, subjected to limited protease digestion with various proteases as indicated.

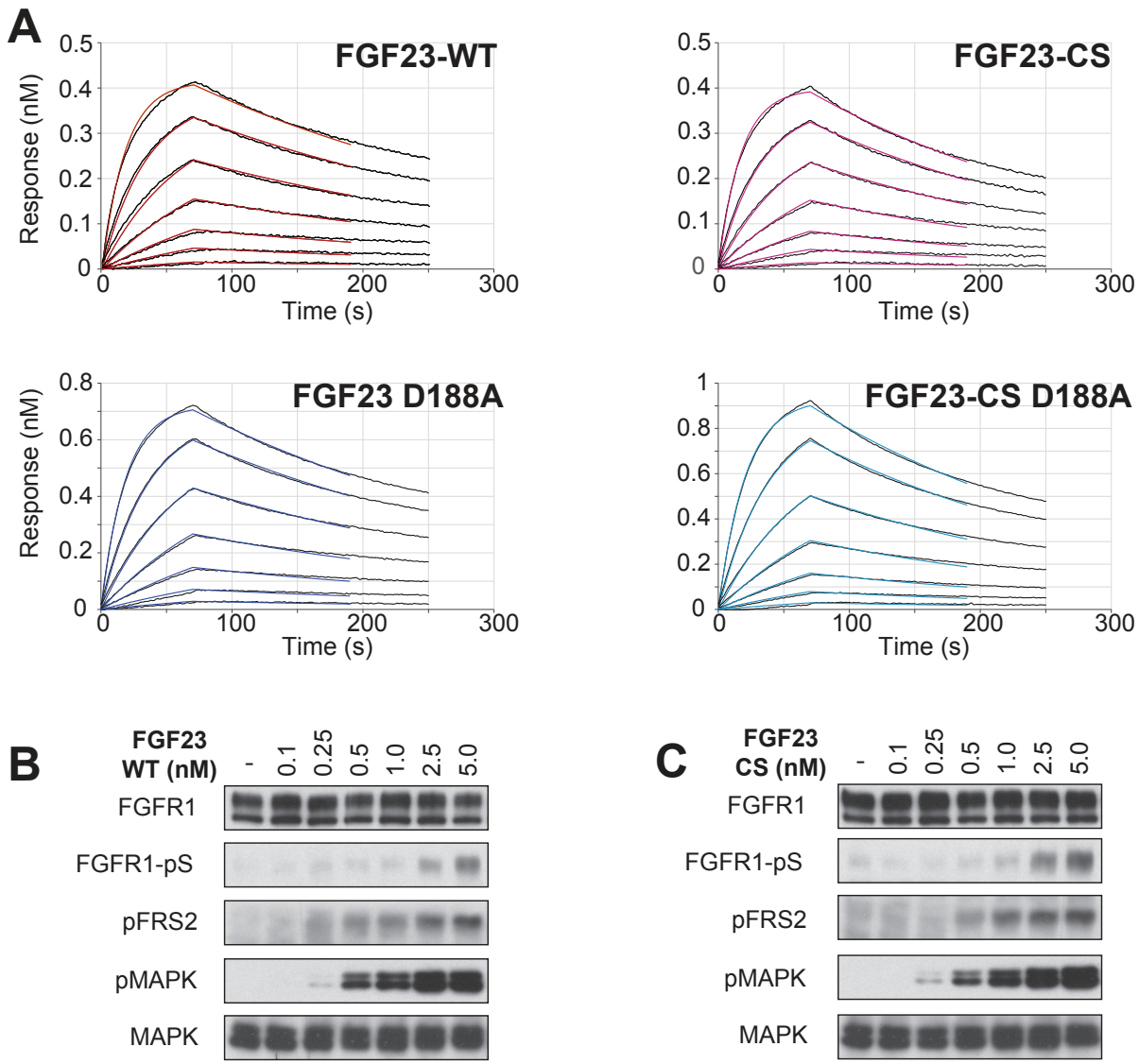

Figure S6.
FGF23-WT and FGF23-CS bind α-Klotho with similar affinities and activate cell signaling to a similar extent. **A.** BLI sensorgrams for the binding of FGF23-WT, FGF23-CS, FGF23 D188A and FGF23-CS D188A to sKLA. Biosensors coated with anti-mouse-Fc antibody was used to immobilize anti-Flag antibody followed by capturing Flag-tagged FGF23-WT or FGF23-CS. Biosensors were then dipped into solutions containing a series of concentrations of sKLA (200, 100, 50, 25, 12.5, and 6.25 nM). The resulting BLI sensorgrams were fitted with a 1:1 ligand:receptor binding model (colored lines) to calculate kinetic parameters and dissociation constants. **B and C**. HEK293 cells stably expressing FGFR1c together with α-Klotho were left unstimulated or stimulated with increasing concentrations of FGF23-WT or FGF23- CS mutant, as indicated, for 10 minutes at 37°C. Cell lysates were subjected to SDS-PAGE and analyzed for serine phosphorylation of FGFR1, tyrosine phosphorylation of FRS2 and for MAPK activation by immunoblotting with anti-FGFR1-pS, anti-pFRS2 and anti-pMAPK antibodies, respectively and with anti-MAPK as a control.

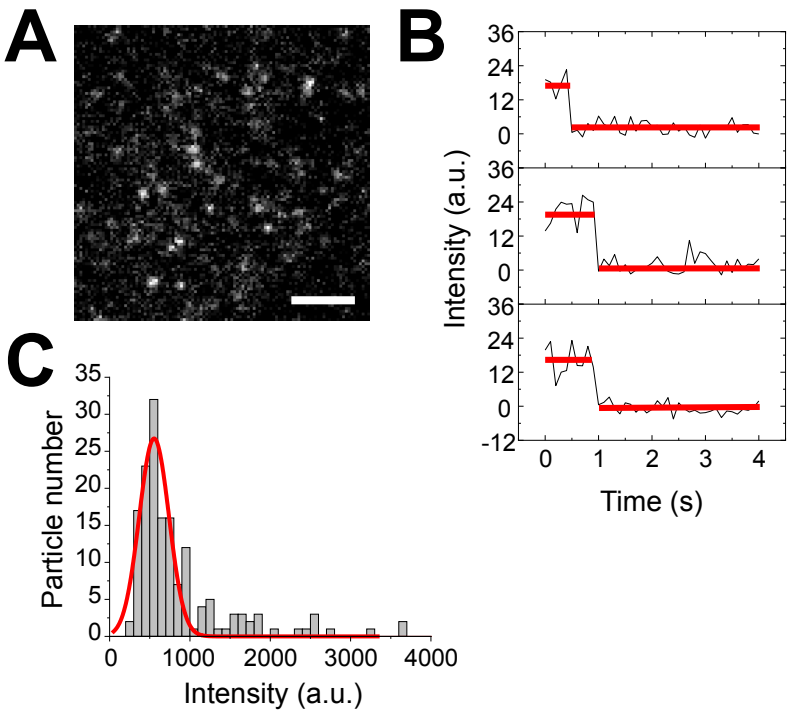

Figure S7.
Detection of single molecules of free Alexa488 HaloTag ligand by TIRFM. **A.** TIRFM image of Alexa488 HaloTag ligand spotted onto glass. Scale bar, 2.5 μm. **B.** Representative single-step photobleaching of Alexa488 HaloTag ligand particles. Average fluorescence intensity within a 0.55-μm-diameter region surrounding a particle was measured with local background subtraction (using a concentric annulus) and plotted against time. Note similar intensity of the three examples before and after bleaching (red). **C.** Intensity distribution of Alexa488 HaloTag ligand particles. The distribution was best fitted with a single Gaussian (red curve). For intensity distribution analyses, intensities were calculated by fitting the fluorescence of particles with 2D Gaussian functions and taking the volume under the fit.

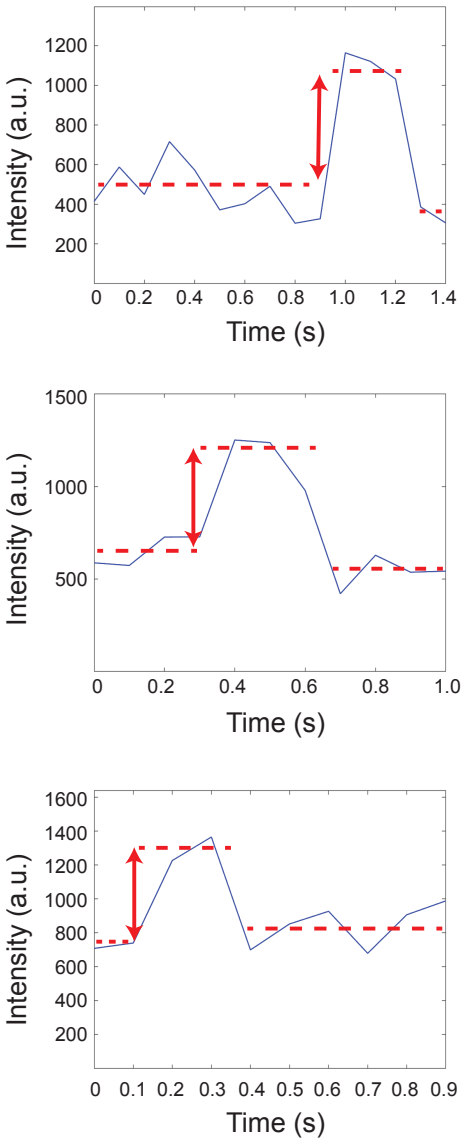

Figure S8.
Examples of intensity changes of individual tracks of HaloTag-α-Klotho particles compatible with reversible dimer formation. Arrows highlight the abrupt doubling of particle intensity. The starting intensity likely corresponds to that of a single molecule, based on the intensity distribution of particles (Fig. 4D). Representative single-step photobleaching of HaloTag-α-Klotho particles. Average fluorescence intensity within a 0.55-μm-diameter region surrounding a HaloTag-α-Klotho particle was measured with local background subtraction (using a concentric annular region with inner and outer diameters of 0.55 and 1.1 μm, respectively) and plotted against time. Note similar intensity of the particles before bleaching (highlighted by red lines).

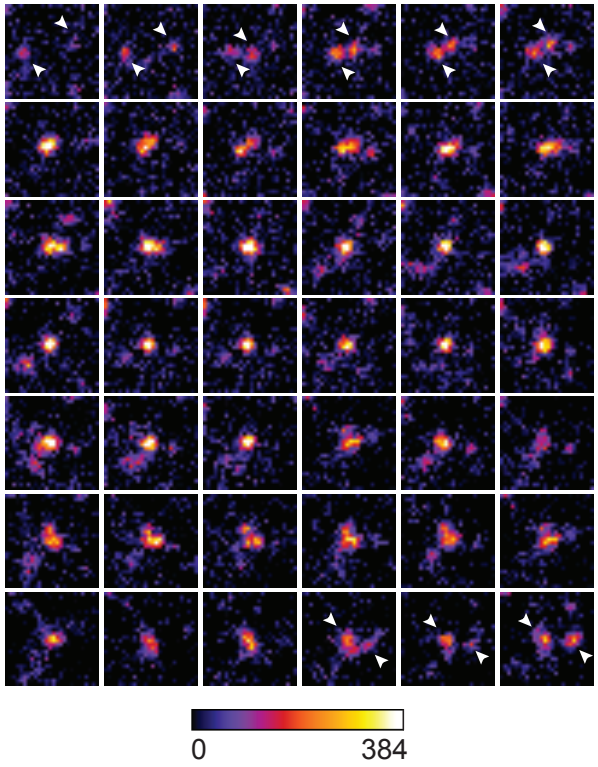

Figure S9.
Example of HaloTag-α-Klotho particles transiently merging. Image sequence of consecutive frames showing two monomers (arrowheads) diffuse towards each other, merge and then dissociate back into monomers. Color lookup table (bottom).

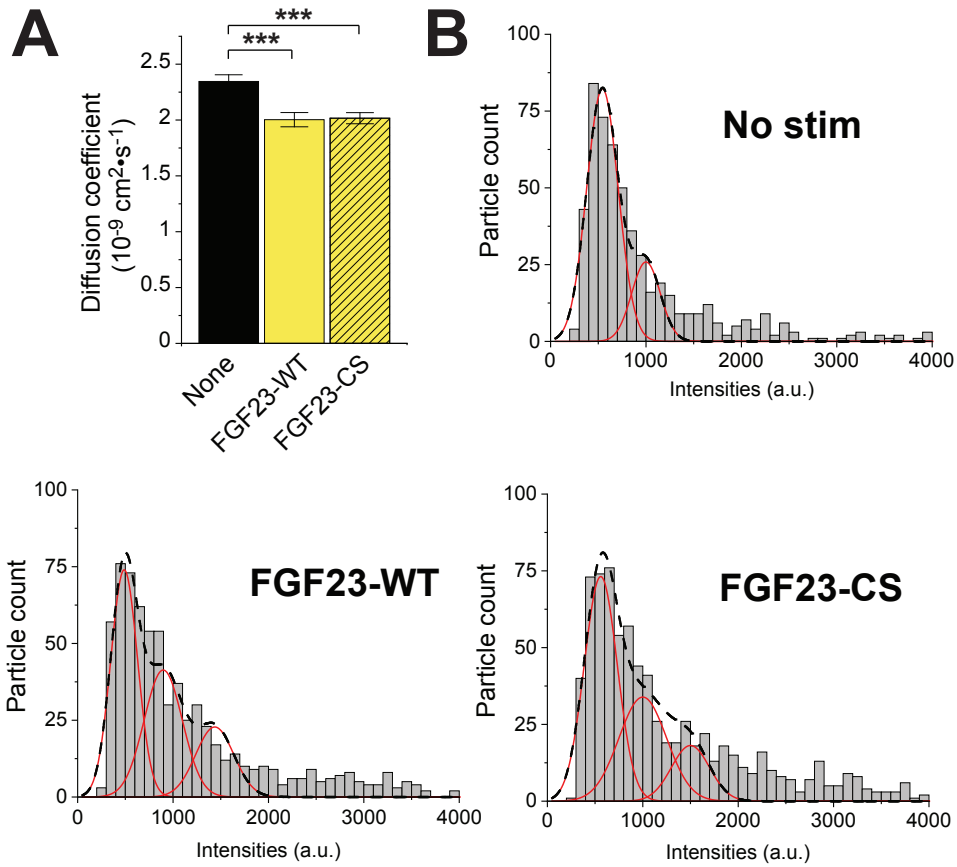

Figure S10.
FGF23-WT and its CS mutant similarly dimerize Klotho molecules on cell membranes. **A.** Diffusion coefficient of HaloTag-α-Klotho particles calculated from their mean square displacement in unstimulated cells (12 cells, 2 transfections) and cells stimulated with mammalian produced FGF23-WT (25 nM; 14 cells, 2 transfections) or FGF23-CS (25 nM; 14 cells, 2 transfections). Error bars indicate mean±s.e., ***P<0.0001 by Student's t-test. **B.** Representative intensity distributions of HaloTag-α-Klotho in a cell left unstimulated (top panel) or stimulated with mammalian produced FGF23-WT or FGF23-CS for ~10min (bottom two panels). Intensities represent the volume of 2D Gaussian fits of the fluorescence of particles. Intensities were taken from the beginning (3 frames) of each recording and their distribution was fitted with a mixed Gaussian model. Black dashed lines, mixed fit. Red lines, individual components.